RSC Advances

PAPER

View Article Online
View Journal | View Issue

Cite this: *RSC Adv.*, 2014, **4**, 58287

Synthesis and characterization of a poly(ethylene glycol)–poly(simvastatin) diblock copolymer

Theodora A. Asafo-Adjei,[a] Thomas D. Dziubla[b] and David A. Puleo*[a]

Biodegradable polyesters are commonly used as drug delivery vehicles, but their role is typically passive, and encapsulation approaches have limited drug payload. An alternative drug delivery method is to polymerize the active agent or its precursor into a degradable polymer. The prodrug simvastatin contains a lactone ring that lends itself to ring-opening polymerization (ROP). Consequently, simvastatin polymerization was initiated with 5 kDa monomethyl ether poly(ethylene glycol) (mPEG) and catalyzed *via* stannous octoate. Melt condensation reactions produced a 9.5 kDa copolymer with a polydispersity index of 1.1 at 150 °C up to a 75 kDa copolymer with an index of 6.9 at 250 °C. Kinetic analysis revealed first-order propagation rates. Infrared spectroscopy of the copolymer showed carboxylic and methyl ether stretches unique to simvastatin and mPEG, respectively. Slow degradation was demonstrated in neutral and alkaline conditions. Lastly, simvastatin, simvastatin-incorporated molecules, and mPEG were identified as the degradation products released. The present results show the potential of using ROP to polymerize lactone-containing drugs such as simvastatin.

Received 12th September 2014
Accepted 30th October 2014

DOI: 10.1039/c4ra10310f

www.rsc.org/advances

Introduction

The use of biodegradable polymers in therapeutic applications has grown due to their favorable characteristics, which include biocompatibility, tailorable degradation, and the ability for some polymer degradation products to be metabolized.[1,2] Poly(glycolic acid) (PGA), poly(lactic acid) (PLA), and poly(lactic-*co*-glycolic acid) (PLGA) are among the earliest biodegradable polyesters to be investigated. Unlike the degradation products of some polyesters, such as poly(ε-caprolactone), glycolic and lactic acid are fully metabolized in the body.[3] Commercial products based on these polymers include PGA/PLA sutures, approved by the FDA in 1971, to PLGA–collagen and PLA meshes and devices on the market for clinical regenerative treatments.[4] These degradable biomaterials can also encapsulate active agents within their matrices or in reservoirs, but polymers have also carried covalently conjugated drugs.[5] Polymer–drug conjugates have been a prevalent method of drug delivery since their conceptual development in 1975 to many different conjugates currently used.[6,7] These systems have used synthetic polymers, such as poly(lysine), poly(glutamic acid), and poly(phosphazene), to bind anti-cancer and anti-inflammatory drugs along their backbone *via* cleavable hydrazone bond linkers.[8,9]

While several characteristics of polyesters are advantageous, promoting their recurrent use in drug delivery, these biomaterials can have a limited capacity to entrap drug.[10,11] Also, if structural or mechanical loading-induced defects exist in coated or drug repository devices, dose-dumping could lead to concentrations high enough for toxic effects to occur.[12–14] Drug conjugation to the polymer backbone can prevent this issue, and it can preserve activity by shielding drugs from degradation as well as prolong drug circulation.[7] However, this system also has the disadvantage of limited linkages available for drug loading.[9]

Incorporation of drug into the polymeric backbone, such as the degradable aspirin-derivatized poly(anhydride ester)[15] and poly(trolox ester) polymers[16] developed for anti-inflammatory and antioxidant therapeutic applications, respectively, circumvents limited drug loading. In these polymers, the weight percentage of drug is increased to nearly 100% as a result of these active molecules essentially being linked to each other to form a macromolecule. The step growth and esterification polymerization mechanisms used to synthesize polydrugs such as the ones mentioned can require multiple reaction steps, however. Little literature exists on using the molecular chemistry of a therapeutic agent to create the backbone of its homopolymer or copolymer *via* ring-opening polymerization (ROP), such as the polymerization of lactonized ricinoleic acid.[17]

ROP has been utilized to polymerize lactones, among many types of cyclic monomers, into their respective polymers. Lactide and glycolide are examples of lactone monomers used to synthesize PLA, PGA, and PLGA *via* ROP, which can be initiated

[a]*Department of Biomedical Engineering, University of Kentucky, 522A Robotics and Manufacturing Building, Lexington, KY, 40506-0108, USA. E-mail: puleo@uky.edu; Fax: +1-859-257-1856; Tel: +1-859-257-2405*

[b]*Department of Chemical and Materials Engineering, University of Kentucky, Lexington, KY, USA*

by metal or organic catalysts to obtain high molecular weight macromolecules.[18] Potential drawbacks that exist in the mechanism include competing depolymerization reactions and other side reactions that can influence the yield and quality of the resulting polymer.[19] However, ROP is versatile in using a range of hydroxyl-containing macromolecules and alcohols to initiate polymerization and alter polymer properties, and minimal steps are usually necessary to develop the polymer. ROP also has the ability to develop high molecular weight chains depending on the type of catalyst and molar ratios chosen for synthesis, which control the number of monomeric units attached. These advantages reveal the usefulness of ROP to create a unique polyprodrug as a biomaterial for drug delivery.

The therapeutic prodrug simvastatin contains a 6-membered lactone ring that is theoretically capable of being opened and reacted to form a polymer *via* ROP, much like monomers of PLA and PGA. Simvastatin is well known as the active ingredient in Zocor, an oral medication for treating hypercholesterolemia. However, the drug also exhibits anti-atherosclerotic, anti-inflammatory, angiogenic, and osteogenic properties in its active hydroxyacid form.[20–23] Different polymeric devices have already explored encapsulation and release of simvastatin for bone regenerative applications.[24–26] Simvastatin is readily metabolized, ensuring removal from the body.[27] Oral administration of statins can cause adverse muscular and hepatic effects[28] that likely are related to the high frequency of large doses needed to overcome first-pass metabolism. Polymerizing simvastatin addresses the issue of dose dumping, removes the need for a bioinert polymeric carrier, and provides the option of increasing the loaded amount of simvastatin while prolonging release at therapeutic concentrations.

The objective of the present studies was to investigate the polymerization of simvastatin using ROP. Reactions were conducted at different temperatures to evaluate the effects of temperature *via* kinetic analysis. The copolymer was also subjected to neutral and alkaline conditions to test degradation *via* hydrolysis.

Experimental

Materials

Simvastatin was purchased from Haouri Pharma-Chem (Edison, NJ). Tin(II) ethylhexanoate (stannous octoate), monomethyl ether poly(ethylene glycol) (mPEG), anhydrous toluene, anhydrous diethyl ether, dichloromethane (DCM), and deuterated chloroform ($CDCl_3$) were purchased from Sigma-Aldrich (St. Louis, MO). Tetrahydrofuran (THF) stabilized with 3,5-di-*tert*-butyl-4-hydroxytoluene (BHT) was purchased from Fisher Scientific (Pittsburgh, PA).

Methods

Poly(ethylene glycol)-*block*-poly(simvastatin) synthesis. Approximately 400 mg microscale reactions of simvastatin (400 mg, 0.956 mmol) and mPEG (47.8 mg, 9.56 μmol) were performed to assess reaction kinetics using a procedure adapted from the literature.[29] All reactions were performed at 150 to 250 °C in a silica sand bath for improved temperature control. Internal solution temperatures were found to be 10 to 20 °C lower than the sand bath temperatures. The reactant components were dried at 130 °C in a nitrogen atmosphere for 1 h followed by the reaction temperature for an additional hour. Samples for the initial time point were taken after the reactants melted into a homogenous bulk mixture and before catalyst addition. After the drying period, 1 wt% of stannous octoate dissolved in toluene was added to the melt by syringe. Each reaction ran for 24 h, with three samples taken at each of 0, 1, 4, 8, 12, 18, and 24 h. The theorized reaction scheme is shown in Fig. 1a.

A macroscale synthesis of the diblock copolymer (2.5 g) was performed at 230 °C for 24 h with the same reaction conditions described in the preceding paragraph. The crude product was purified by vacuum filtration after obtaining the precipitate using DCM as the solvent and cold diethyl ether in excess as the anti-solvent to further remove any residual monomer. Simvastatin (0.4 g) with and without catalyst addition was heated at 240 °C for 24 h to assess the effect of temperature on its molecular weight.

Gel permeation chromatography (GPC). Molecular weight was measured using a Shimadzu Prominence LC-20 AB HPLC system with a Waters 2410 refractive index detector. Two 300 × 7.5 mm, 3 μm particle size ResiPore columns (Agilent Technologies) in series were used for sample separation. Samples were injected using THF as the eluent at a 1.0 ml min^{-1} flow rate. Standard curves were prepared using polystyrene standards ranging from 160 Da to 370 kDa. Shimadzu Lab Solutions software was used to calculate weight (MW) and number-average molecular weight (M_n) and the polydispersity index (PDI, MW/M_n). Simvastatin monomer conversion (*i.e.*, molecular weight growth of the poly(simvastatin) block) was determined as a function of time.

Nuclear magnetic resonance (NMR) spectroscopy. H-NMR spectra were developed from Varian Gemini NMR 400 MHz spectrometers connected to a VnmrJ software interface. Samples of the copolymer and a melted mixture of simvastatin and mPEG (100 : 1 molar ratio) weighing 5 to 7 mg each were dissolved in 1 ml of $CDCl_3$, transferred into NMR sample vials and analyzed for additional structure characterization.

Fourier transform infrared (FTIR) spectroscopy. Spectra were obtained using a Varian FTS-7000e FTIR spectrophotometer with a 0.25 cm^{-1} resolution. Samples weighing 3 to 5 mg were placed directly onto a germanium attenuated total reflectance crystal and compressed for analysis. The functional groups of the copolymer (synthesized at 230 °C) were compared to those found in a melted mixture control of simvastatin and mPEG, as well as the components individually. Peak locations and heights of stretches characteristic of simvastatin and mPEG were identified and compared between the copolymer and its controls.

***In vitro* degradation.** Small 16 to 18 mg disks were made by dissolving polymer in DCM (60 wt%) and pipetting the solution onto a Teflon plate to evaporate the solvent overnight. Disks were placed in 3 ml of 1 M NaOH (aq) or phosphate-buffered saline, pH 7.4 (PBS). Disks were weighed and medium was

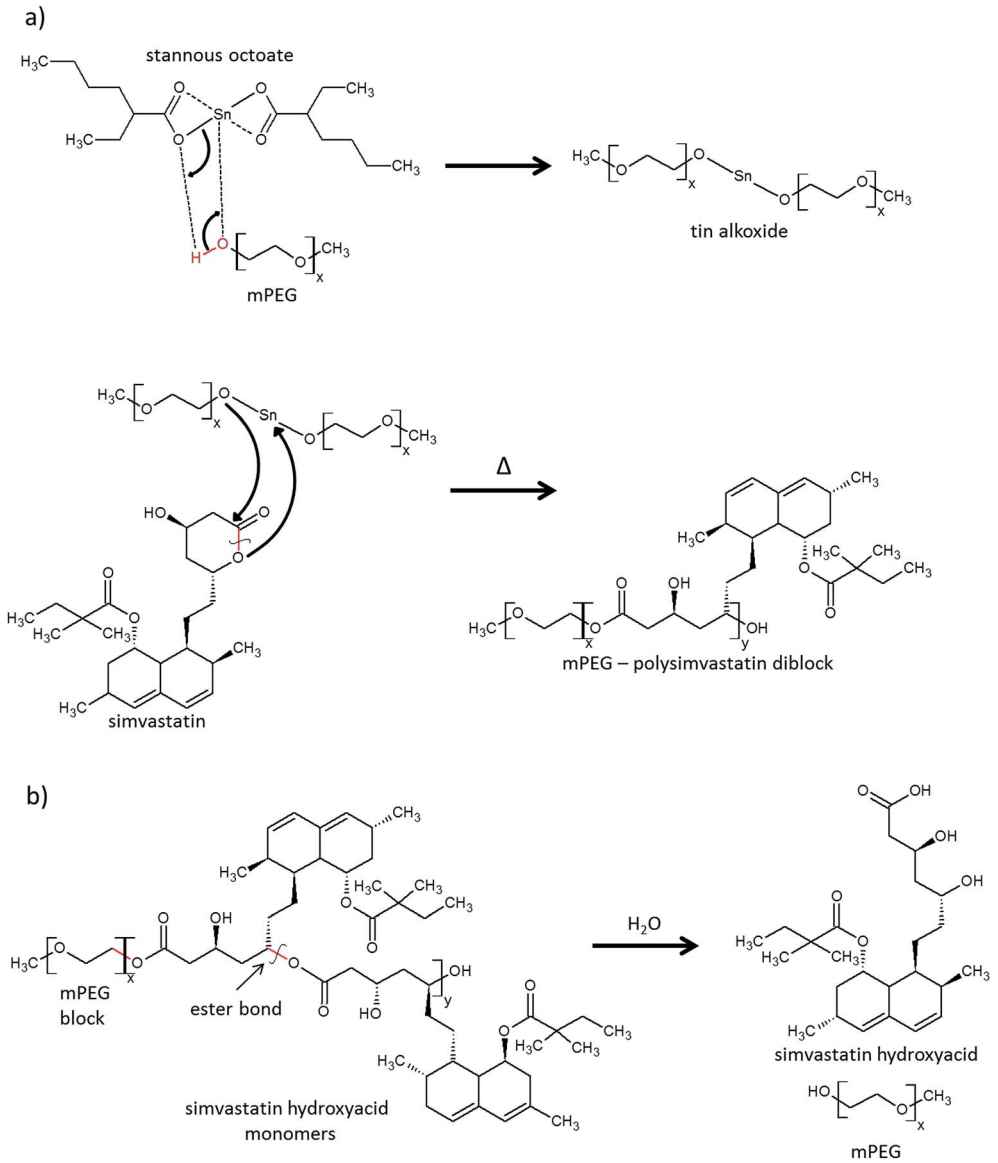

Fig. 1 (a) Tin alkoxide complex formation and proposed mechanism of ROP reaction to form poly(ethylene glycol)-*block*-poly(simvastatin). (b) Proposed mechanism of hydrolytic degradation of the copolymer.

completely replaced at each time interval. Total dry weight of the disks was measured at 2 and 6 weeks. Aliquots were retrieved at intervals and analyzed for absorbance at 240 nm using a PowerWave HT microplate spectrophotometer with a Gen5 analysis software interface. The theorized mechanism of degradation is shown in Fig. 1b.

Matrix-assisted laser desorption/ionization-time of flight mass spectrometry (MALDI-TOF MS). Degradation supernatants were analyzed for product identification, relative abundance of different products, and molecular weight distribution using a Bruker Ultraflextreme MALDI-TOF MS in positive ion mode. This instrument provides a smartbeam-II solid state laserbeam (355 nm) focus as low as 10 μm for quality spatial resolution, speed of up to 2 kHz, and a detector with a resolving power and mass accuracy of 40 000 and 1 ppm, respectively. Samples of simvastatin, mPEG, and degraded products in PBS were lyophilized and then solubilized in THF. The sample solutions were then centrifuged at 2500 rpm for 3 min to remove the undissolved salts. The remaining supernatants containing the dissolved compounds were syringe filtered (0.45 μm) before analysis. Approximately 1 μL of each sample solution was analyzed on a stainless steel target. Alpha-cyano-4-hydroxycinnamic acid (CHCA) was used as the matrix.

Statistical analysis. Two-way ANOVA with a Bonferroni post-test was performed on the kinetic data to test the effects of reaction time and temperature on molecular weight growth of the copolymer and the effects of degradation time and pH on simvastatin release from the copolymer. An unpaired student *t*-test was conducted to test for differences between means of mass lost. Values of $p < 0.05$ were deemed statistically significant. Data were plotted as mean and standard deviation.

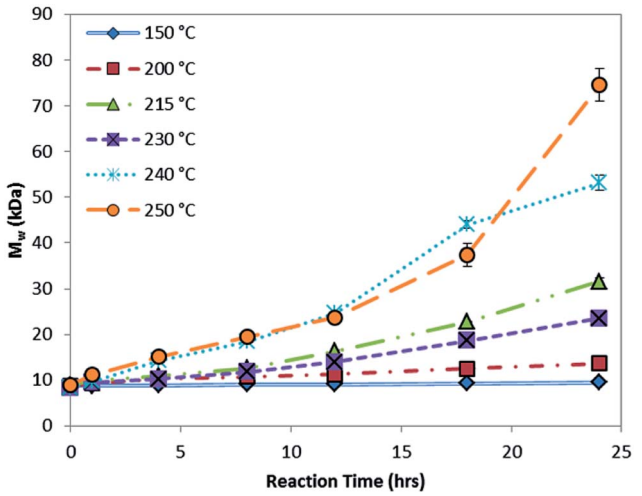

Fig. 2 MW of copolymer during ROP at increasing temperatures. Simvastatin and mPEG (5 kDa) were mixed at a 100 to 1 molar ratio for each reaction. The 0 h time point represents the MW of mPEG before poly(simvastatin) chain growth. The GPC molecular weight of mPEG registered higher than its theoretical value due to differences in chemistry between mPEG and the polystyrene standards used. Data are mean ± standard deviation ($n = 3$).

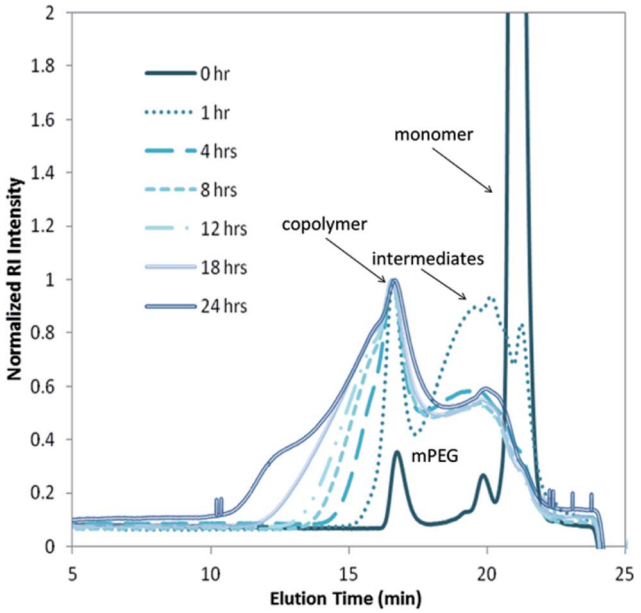

Fig. 3 GPC chromatogram showing monomer (simvastatin) attachment to the mPEG block to form copolymer at 250 °C. Chromatograms were normalized to the copolymer peak. The 0 h mPEG and simvastatin peaks are excluded from normalization due to the monomer peak registering at a high intensity (6.4).

Results

Synthesizing poly(ethylene glycol)-*block*-poly(simvastatin) at 150 °C and above generated crude copolymers that increased in MW with time (Fig. 2). At 150 °C, a minimal MW of 9.5 kDa was observed, which correlated to approximately two simvastatin monomers in each chain. However, as the temperature of reaction increased above 200 °C, polymer growth increased significantly, reaching poly(simvastatin) chain lengths of 19 to approximately 260 monomeric units attached to an mPEG block. The latter corresponded to a MW of 74 kDa formed at 250 °C. The kinetics of the temperature-dependent reactions fitted best to a first-order rate model,

$$\mathrm{MW}_t = \mathrm{MW}_\mathrm{o} e^{-kt} \quad (1)$$

where MW_t is molecular weight at time t, MW_o is initial molecular weight, and k is the rate constant (Table 1). Reactions run at 150 and 200 °C showed significantly lower rates of MW growth, with constants of 0.0033 and 0.0169 h^{-1} (Fig. 2). First-order kinetics became more evident as the temperatures of 215, 230, 240, and 250 °C led to higher rate constants of 0.0052, 0.0042, 0.0782, and 0.0806 h^{-1}, respectively. Regardless of the molecular weight values obtained at each temperature, the M_n values for the crude products did not exceed 13 kDa (Table 1).

Fig. 3 shows a chromatogram depicting the conversion of monomers (*i.e.*, simvastatin, represented by the peak at 22 min) to a larger MW product at 250 °C. A marked decrease in the monomer peak area represented rapid consumption to form intermediate simvastatin-conjugates (17.5 to 21 min). The formation of product with a MW higher than that of mPEG followed. The extended MW growth of the copolymer was represented by a slight leftward shift from the peak of mPEG (17 min) and a broadened shoulder, beginning at 10 min, to the maximum peak height at 16.5 min.

Table 1 Summary of the highest MW obtained, derived rate equation, and percentage in the crude product at each temperature at 24 h

Temperature (°C)	Rate equation	Rate constant (h^{-1})	MW at 24 h (kDa)	M_n at 24 h (kDa)	% in crude product
150	$y = 8.74e^{0.0033t}$	0.0033	9.5	9.1	8.5
200	$y = 9.20e^{0.017t}$	0.017	13.6	10.7	38
215	$y = 8.88e^{0.052t}$	0.052	31.6	13.1	64
230	$y = 8.57e^{0.042t}$	0.042	23.5	12.2	60
240	$y = 9.40e^{0.078t}$	0.078	53.2	11.1	69
250	$y = 9.81e^{0.081t}$	0.081	74.6	10.9	75

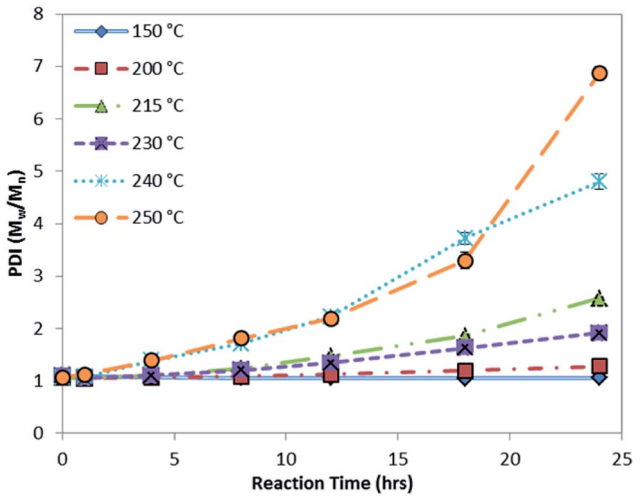

Fig. 4 Changes in PDI at different temperatures of 24 h ROP reactions. The PDI at 0 h represents solely the mPEG block, and the subsequent points reflect addition of simvastatin monomers. Data are mean ± standard deviation ($n = 3$).

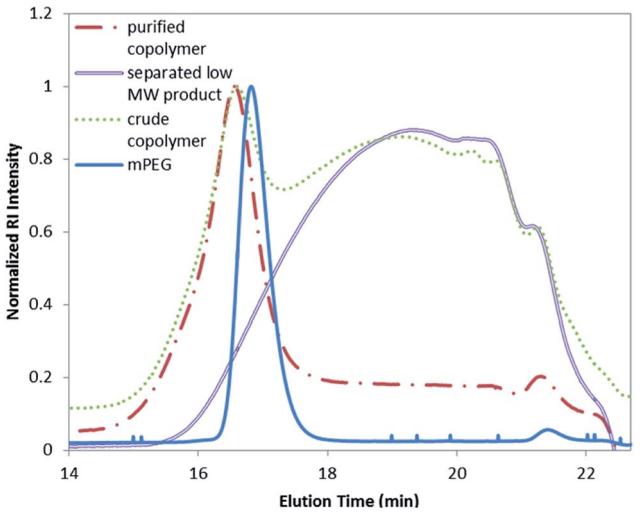

Fig. 5 GPC chromatogram of separated products after purification of the crude copolymer.

The PDIs corresponding to the MW kinetics are shown in Fig. 4. At 150 °C, where minimal molecular weight growth was seen, the PDI remained at 1.05 after 24 h. However, at 200 and 230 °C, the values increased up to 1.3 and 1.9, respectively. PDIs reached 4.8 and 6.9 at the highest temperatures of 240 and 250 °C, respectively.

Further characterization of copolymer purification is shown by a GPC analysis of the crude product and the resulting retentate (desired copolymer) and filtrate (lower molecular weight products) (Fig. 5). The copolymer peak after separation was seen at an elution time of 16.5 min. Intermediate products and unreacted simvastatin, represented by the elution time range of 18 to 22 min in Fig. 3, were removed from the crude copolymer by subsequent vacuum filtration. The vacuum filtration step isolated the purified copolymer product in the retentate.

Analyzing the rate of propagation and the process by which the simvastatin monomer converted to copolymer at high temperatures led to heating the monomer, with and without the catalyst, at 240 °C to assess effects in the absence of mPEG as the initiator. Interestingly, heating simvastatin alone and simvastatin with catalyst produced molecular weights of 10 ± 4.7 kDa and 14 ± 11 kDa with PDIs of 2.3 ± 1.5 and 4.7 ± 2.5, respectively. Both products still had lower MW values than the product obtained in the high temperature copolymer reaction at 240 °C, which was 53 kDa with a PDI of 4.8. The majority of the conjugation produced was represented by the intermediate simvastatin product peaks, shown in Fig. 3, most of which did not appear after purification (Fig. 5, Table 2).

NMR spectra of the monomer and copolymer synthesized at 230 °C are shown in Fig. 6. Integration measurements showed approximately 38 simvastatin monomers attached within the poly(simvastatin) block in the sample. Simvastatin has a molecular weight value of 418.57 Da, which led to a calculated MW of 21 kDa, similar to the MW seen in the kinetics analysis at 230 °C.

FTIR analysis of the functional groups of the synthesized copolymer is shown in Fig. 7. Comparing the copolymer spectrum to the spectra of simvastatin and a mixture of simvastatin and mPEG revealed a carbonyl (–C=O) band shift from 1704 cm^{-1} to 1722 cm^{-1}. An increase in the intensity

Table 2 Summary of product MW distributions from purification, measured *via* GPC

Sample	Component	MW (kDa)	Composition (%)	Yield (%)
Crude copolymer	Highest MW	11.5	28	—
	Intermediates	2.1	48	
	Monomer	0.3	24	
Purified copolymer	Highest MW	10.2	87	18
	Intermediates	0.4	6.2	
	Monomer	0.2[a]	6.8	
Separated low MW weight product	Intermediates	3.2	66	—
	Monomer	0.3	34	

[a] The GPC calibration curve has greater error for molecules with theoretical molecular weight values below 0.5 kDa, which may explain why the value for simvastatin monomer is not consistent in the table and why the value registers lower than the molecular weight value of 418.57 Da.

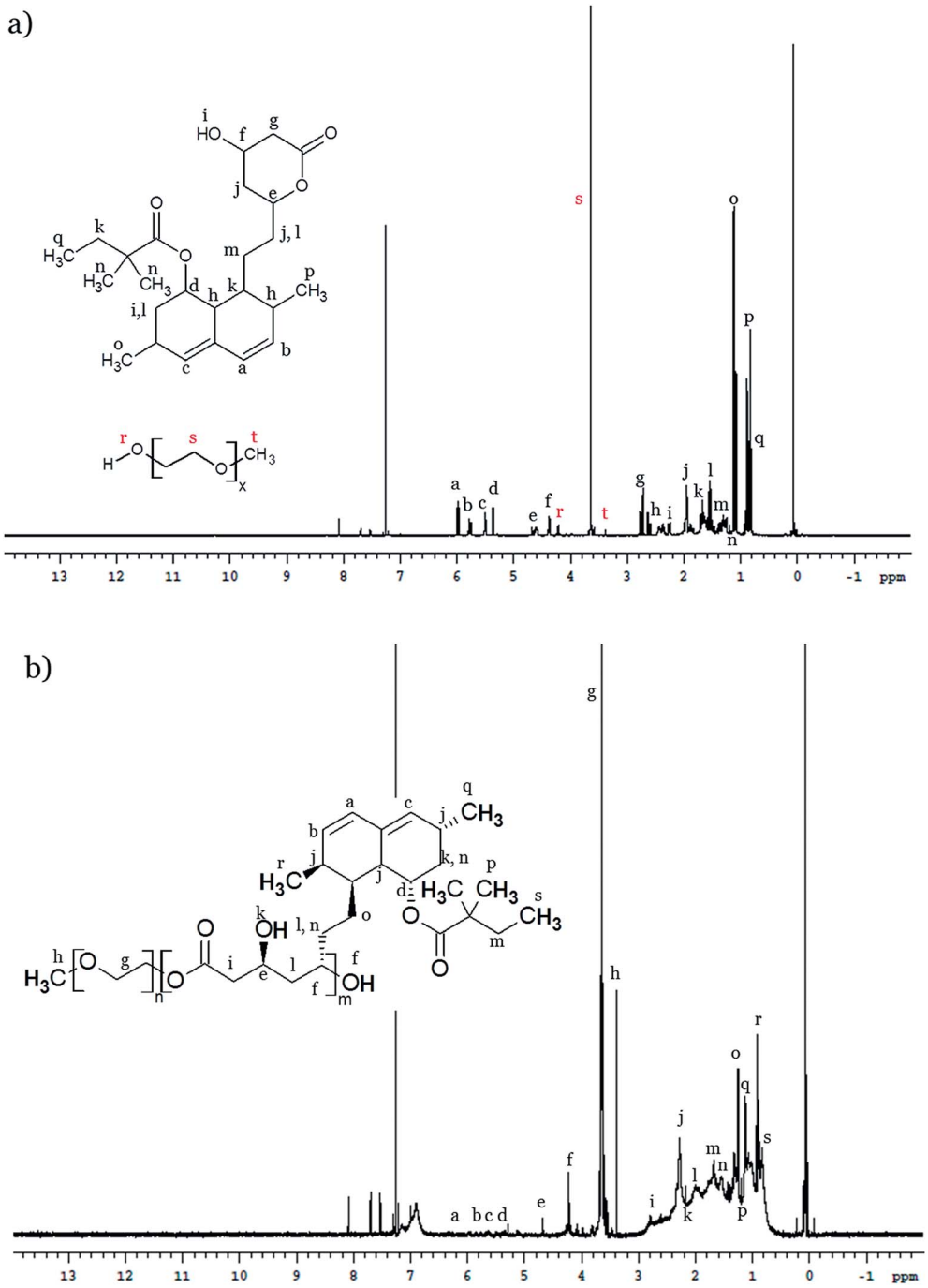

Fig. 6 H-NMR spectra in $CDCl_3$ (7.25 ppm) of: (a) simvastatin and mPEG mixed at a 100 : 1 molar ratio and (b) poly(ethylene glycol)-*block*-poly(simvastatin).

ratio of the –CH–CH– (2900–3000 cm^{-1}) to –C═O bands was seen in the copolymer spectrum compared to the control mixture. The copolymer spectrum also exhibited stretches characteristic of both simvastatin and mPEG, with the carbonyl band at 1722 cm^{-1} and the methyl ether band of mPEG at 1096 cm^{-1}.[30,31]

Mass loss and drug release of the disks in PBS and 1 M NaOH are shown in Fig. 8. Over the first two weeks, water uptake by the samples led to an average maximum mass four and three times the initial mass for incubation in PBS and NaOH, respectively. The dry weights decreased 11 and 14% in the PBS and NaOH, respectively, during this time. At 6 weeks, the wet masses were 102 and 68% of the initial mass for PBS and NaOH, respectively, and the dry masses were 13 and 21% lower. The dry mass loss for the NaOH group had a larger mean decrease compared to samples in PBS, but the difference was not significant. The

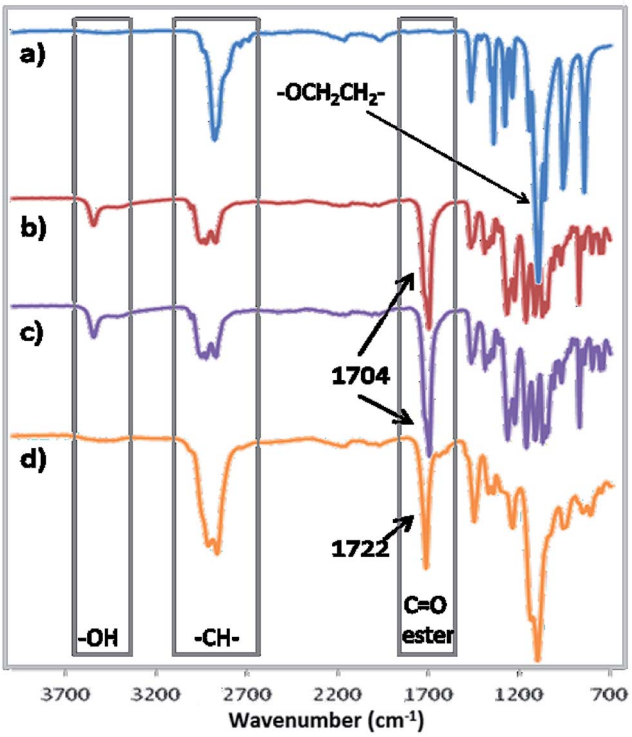

Fig. 7 FTIR spectra of: (a) mPEG, (b) simvastatin, (c) simvastatin and mPEG blended at the same molar ratio used for the reaction (100 : 1), and (d) poly(ethylene glycol)-*block*-poly(simvastatin).

cumulative amounts of drug released were 108 and 266 μg in PBS and NaOH, respectively. After an initial burst of 59 μg in 24 h, a zero-order release rate was observed in NaOH with a constant of 7.4 μg h^{-1} between 1 and 10 days. A first-order release rate followed, with a constant of 21 μg per day for the remainder of the degradation period. In PBS, after an initial burst of 37 μg in 24 h, only 2.5 μg was released during the following 8 days. A zero-order release constant of 2.1 μg per day was determined for the remainder of the degradation period. The amounts of simvastatin released in PBS and NaOH were significantly different at day 2 ($p < 0.05$), day 3 ($p < 0.01$), day 4 ($p < 0.001$), and days 5 to 44 ($p < 0.0001$).

Mass spectral data identifying different species of degradation products are shown in Fig. 9. The mass spectrum of simvastatin shows a peak of the highest abundance at 441 mass-to-charge ratio (m/z), simvastatin's ion or the parent ion, and another distinct peak at 702 m/z (Fig. 9a). The mPEG mass spectrum displayed a bell-shaped distribution of peaks, with the highest relative abundance at 5207 m/z, which corresponds well with the theoretical molecular weight of the mPEG used for synthesis (Fig. 9b). Within the low molecular weight spectrum of the degradation products released (Fig. 9c), the 441 m/z peak is present along with a peak at 460 m/z among a multitude of distinct peaks ranging from 490 to 1062 m/z to the right of the parent ion and 385 to 430 m/z to the left. The high molecular weight spectrum of degradation products had a shape similar to that of mPEG, but with a

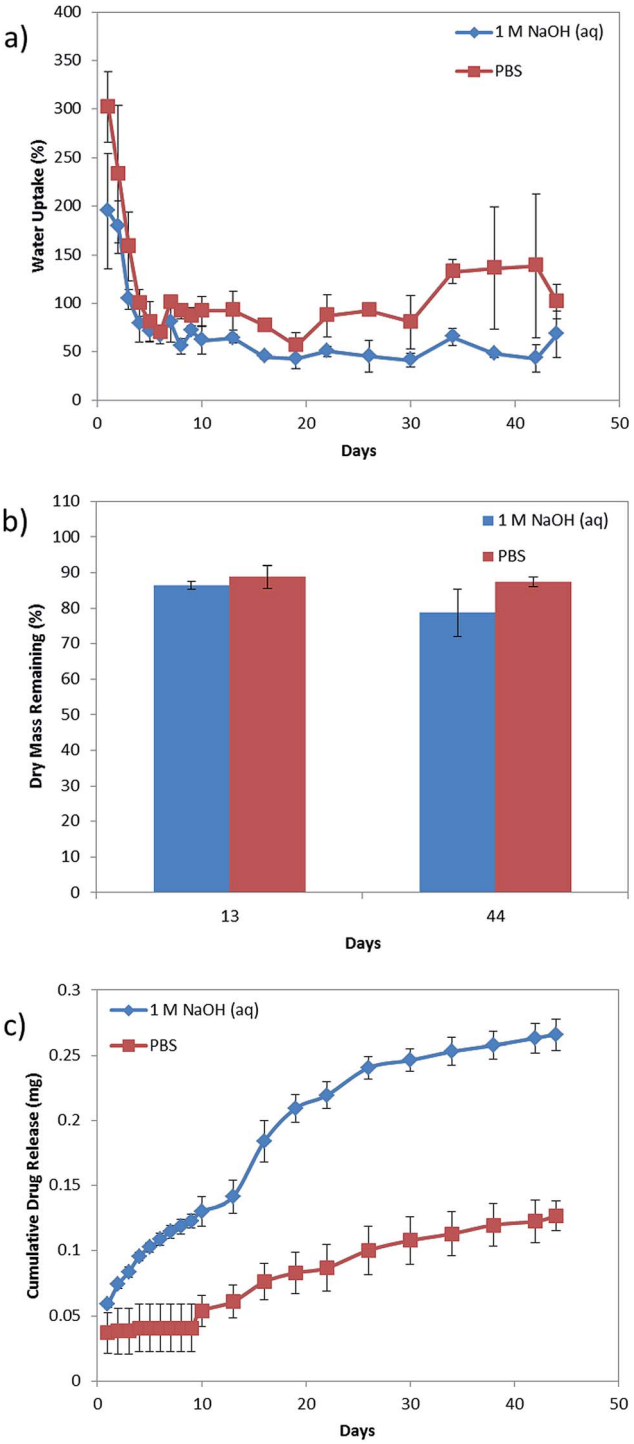

Fig. 8 Degradation and drug release during incubation of samples in PBS or 1 M NaOH. (a) Wet mass, (b) dry mass loss, and (c) drug release. Data are mean ± standard deviation.

rightward shift, and the most abundant ion was at 5312 m/z (Fig. 9d). Although present, the intensity of the 441 and 460 m/z peaks was approximately 50, 35, 60, 50, and 35% of that for ions at m/z of 402, 430, 551, 920, and 5312, respectively, which were the most abundant peaks representing the degradation products.

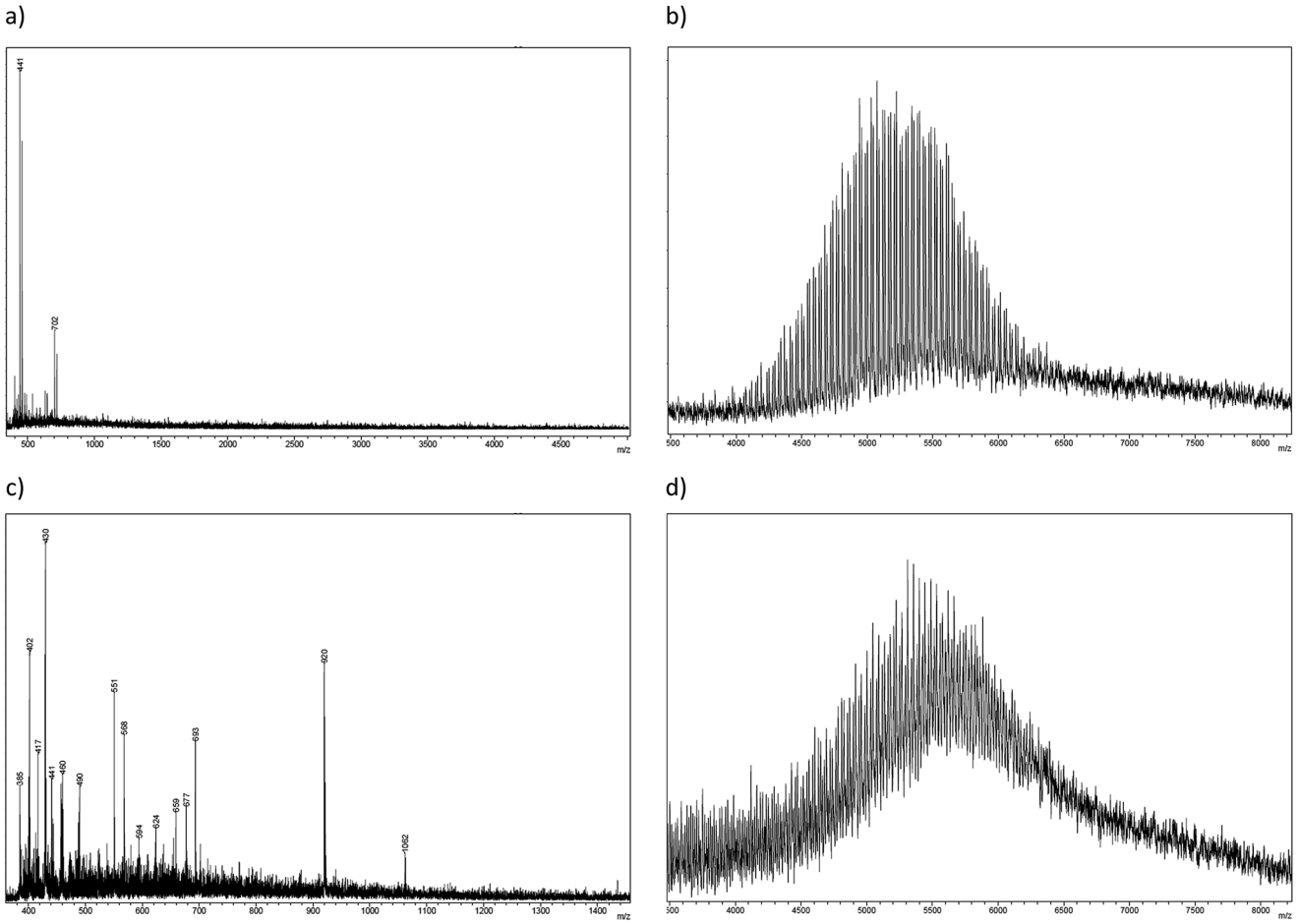

Fig. 9 Mass spectra of (a) simvastatin, (b) mPEG (5 kDa), (c) low molecular weight degradation products, and (d) high molecular weight degradation products.

Discussion

Copolymer characteristics

The molecular and therapeutic properties of simvastatin are desirable for investigating the synthesis of a novel degradable poly(ethylene glycol)-*block*-poly(simvastatin) copolymer for its potential use in drug delivery. Different derivatives of poly(ethylene glycol), which include mPEG, have been used as initiators for the synthesis of block copolymers due to their reactive hydroxyl end groups, biocompatibility, and ability to increase the solubility of hydrophobic counterparts.[32] Reacting simvastatin with mPEG *via* ROP can lead to a simple one-step synthesis of a polyprodrug with unique characteristics. The reaction takes advantage of simvastatin being a prodrug, changing its closed-ring form into monomeric units of its active hydroxyacid, the opened-ring form of simvastatin (Fig. 1a). The ester bond initially in the lactone ring of simvastatin would be embedded in the backbone of its polymer as a result of opening the ring. Thus, polymer degradation and drug release would occur by the hydrolysis of labile ester bonds, allowing the copolymer to degrade into biomolecules of simvastatin hydroxyacid and mPEG (Fig. 1b). These components are metabolized in the liver and excreted by the kidneys, respectively.[33]

Polymerization mechanism

Lactone-based molecules, such as glycolide, lactide, ε-caprolactone, and their combinations, have been used as monomers for the synthesis of PLGA, PLA, and other aliphatic polyesters.[34–36] Like these molecules, simvastatin possesses a lactone moiety capable of chemically opening and developing into a polymer block by the ROP mechanism using stannous octoate, a well-known tin metal catalyst. Aluminum and yttrium isopropoxide (metallic), porcine pancreatic and candida antartica lipases (enzymatic), and various carboxylic acids and amines in the presence of an alcohol (organic) have also been used as catalysts, which in turn dictate the ROP mechanism that occurs.[37] The mechanism of stannous octoate is pseudo-anionic coordination-insertion ROP.[37,38] The metal catalyst first forms a complex with the hydroxyl group of the initiator to form an alkoxide. The more reactive alkoxide begins chain propagation by coordinating with the lactone ring of the monomer, followed by "insertion" of the ring into the alkoxide's metal–oxygen bond.[37,39] Throughout the process, the alkoxide acts as a nucleophile by attacking the carbon of the ring's carbonyl group, leading to cleavage of the acyl bond and extended chain formation with its end bonded to the alkoxide, which is

otherwise known as a living polymerization.[39] A 5 kDa mPEG was used in the synthesis of the present polymers so only one reactive hydroxyl group would be available for propagation of the poly(simvastatin) chain, creating a diblock copolymer.

Kinetic analysis

It was necessary for simvastatin to be in a fluid-like state to ensure homogeneous mixing of all components. This state was possible only above 138 °C, the melting point of simvastatin,[40] hence the high temperature range chosen for conducting melt condensation reactions. However, insignificant growth was seen for the lowest temperature reaction. The same results were also seen for preliminary reactions attempted using tin(II) trifluoromethyl sulfonate, and lanthanum and aluminum isoproproxide at 150 °C and *Candida antarctica* lipase B at 80 °C in toluene (data not shown). Unlike glycolide and lactide, in which the cyclic lactone is their main structure, the lactone ring of simvastatin represents only a portion of the molecule. The other aromatic moieties of simvastatin may interfere with opening the six-membered lactone ring. Lactones of this size also have relatively lower ring strain than do smaller lactones, but their strain is still favorable for polymerization.[41] This characteristic contrasts with the cyclohexane counterpart of the lactone ring of simvastatin that does not polymerize due to the stable chair conformation it assumes without the ester group present.[42] Thus, minimal chain growth between 150 and 200 °C may be due to a combination of ring strain and steric hindrance resulting from the bulky side groups attached to the targeted lactone ring of simvastatin, contributing to a lower than necessary reactivity.

Evidently, the simvastatin to mPEG molar ratios present in the 240 and 250 °C reaction products exceeded the initial 1 to 100 molar ratio in the melt. This finding may indicate low mPEG participation in the reaction and increased interactions between neighboring simvastatin molecules due to the higher weight percentage of the molecule within the bulk reaction mixture. In addition to mPEG having a hydroxyl group able to serve as the active group for initiation, simvastatin also possesses a secondary hydroxyl group attached to its lactone ring, which was unprotected during these reactions. Secondary hydroxyl groups are less reactive than their primary counterparts.[43] Regardless, this available hydroxyl may have allowed chain propagation among the monomeric units to create extensively branched chains before interaction with mPEG to create the diblock copolymer. Simvastatin would then be considered a bifunctional latent AB_2 monomer capable of both initiating ROP, *via* the hydroxyl group on its lactone ring, and chain propagation through the opening of its lactone ring.[44,45] Mevalonolactone, a molecule structurally similar to simvastatin, has been used as a monomer for synthesizing branched copolymers.[45] Bifunctionality of the monomer can lead to a dendrimeric architecture of the copolymer, and in this case, it can lead to the synthesis of linear-hyperbranched mPEG-*block*-poly(simvastatin) copolymer chains fully capable of exceeding the initial 1 to 100 mPEG to simvastatin molar ratio, as more simvastatin monomers are added to the branched segments. Also, because simvastatin would be able to compete with mPEG in initiating ROP and is in much greater abundance, more mPEG would likely remain unreacted, which is represented by the low M_n in Table 1. The neighboring monomer interactions and branching may explain why the profiles strayed farther away from achieving a steady state as temperature increased within the given time period. Regardless, the propagation kinetics of the copolymer reaction exhibited first-order rates, which is generally found to be the rate order of bulk ROP *via* insertion-coordination initiators.[46] By comparing the temperature-dependent rate constants as a function of temperature *via* the Arrhenius equation,

$$k = e^{-E_a/RT} \quad (2)$$

where k is the rate constant, R is the universal gas constant, and T is absolute temperature, an activation energy (E_a) of 14.5 kcal mol^{-1} was obtained. The E_a found of the copolymer reaction is slightly lower but comparable to the activation energy of L-lactide undergoing ROP *via* insertion-coordination (19.6 kcal mol^{-1}).[47]

The limited polymer growth below 200 °C indicates how propagation of the simvastatin chain was a more kinetically-driven reaction. The occurrence of ring opening and subsequent propagation depends on the size of the lactone ring, the bulkiness of side groups attached to the ring, and the inclusion or lack of heteroatoms, all of which affect ring conformation.[39] High ring strain increases lactone reactivity and largely contributes to the driving force for ROP. Thus, ROP may result from the loss of enthalpy (H) caused by dissipated ring strain. Even with cyclic monomers of low ring strain, heteroatoms present in the ring can increase the degrees of freedom of the resulting polymer, which increases the entropy (S) of the reaction and drives the reaction towards completion.[19] Also, depending on the reaction conditions used, such as the solvent and states of the monomer and its polymer (*i.e.*, liquid, gas, or amorphous or crystalline solid), the monomer would be limited to: (a) polymerizing above a floor temperature ($+\Delta H$ and ΔS); (b) polymerizing below a ceiling temperature ($-\Delta H$ and ΔS); (c) polymerizing at any temperature ($-\Delta H$, $+\Delta S$); or (d) not polymerizing at all ($+\Delta H$, $-\Delta S$).[48] The MW growth data show an evident floor temperature with polymerization possible above 150 °C under the given the melt condensation conditions. A more obvious indication of the reaction having a floor temperature relates to the high melting point of simvastatin and physical state necessary for the reaction to proceed. Without solvent present in the reaction vessel, polymerization was limited to temperatures above 138 °C.

Polydispersity

Linear polymers made *via* ROP of lactone rings with low ring strain often have broader molecular weight distributions than those made from lactone rings with high strain, a major factor necessary for opening the ring and progressing the formation of a polymer chain.[39] High PDIs may result from reactions such as transesterification, backbiting, or depolymerization. These occurrences can be represented by PDIs up to a value of 2 by the

Flory–Shultz distribution function.[48] Even higher PDI values may represent nonlinear forms of polymerization (*i.e.*, branching). In the present studies, reactions above 200 °C produced higher PDIs, possibly from poly(simvastatin) branching considering that there was low mPEG participation in the reaction. An increased occurrence of side reactions likely contributed to a portion of the synthesized crude copolymer due to substantially increased kinetic rates at high temperatures. Although stannous octoate is an efficient catalyst, it is also known to promote transesterification,[49] which would only be exacerbated at higher temperatures. Uncontrolled side reactions would in turn contribute to higher PDI values.

The PDIs measured represent solely the copolymer peaks. The baseline did not completely return back to its original intensity after the elution of the copolymer peak, indicating that there was still a residual amount of intermediates and unreacted simvastatin remaining in the purified product sample. Further removal would require an additional purification step in the procedure.

NMR analysis

The chemical shifts labeled 'g' and 'h' in the copolymer spectrum represent the mPEG block,[50] while the remaining labeled shifts relate to the poly(simvastatin) block. The broadened peaks that represent simvastatin up-field between 2.91 and 0.067 ppm indicate polymerization that has occurred to form the poly(simvastatin) block. However, the integration ratio of the poly(simvastatin) area upfield (2.91 to 0.067) to the area downfield (7.22 to 6.71, ratio; 17.0) is far from 1, suggesting some sort of degradation or other form of conjugation that may have occurred due to the high temperature of the reaction. The residual side products as a result may explain the shifts seen beyond 6.71 ppm, or they may be an artifact of the environment of copolymer's proposed branched structure.

Functional groups and bond formation

The carbonyl shift shown in the IR spectrum of the copolymer suggested new ester bond formation. The change in height of the –CH–CH– stretch may be a representation of monomer addition (with a –C═O group) to the mPEG block (without a –C═O group). Also, the copolymer spectrum showing stretches characteristic of both components indicated that a chemical bond between the two blocks occurred compared to the mixed control, which showed only peaks characteristic of simvastatin, regardless of the presence of mPEG.

Degradation

The samples in PBS showed an increasing trend in percentage wet mass in the last 3 weeks compared to those in NaOH. An increase in surface area due to disk breakage, despite a minimal loss in dry mass, may have aided in an increased absorption of medium. The high water absorption seen in both groups can also be explained by the presence of the hydrophilic mPEG block of the copolymer. The initial burst and subsequent zero-order release observed may indicate small molecules of free simvastatin and oligosimvastatin close to the sample surface being easily dispersed into the medium with the aid of water absorption by mPEG. The first-order rate seen in the NaOH group may be influenced by the existing concentration of simvastatin in medium or by the scission process in which poly(simvastatin) breaks down into simvastatin, which is only then detectable in solution. Even though 108 to 266 μg of simvastatin were released from the samples during a 6 week period, release of other degradation byproducts, some of which do not have maximum absorption at 240 nm, would account for the remaining mass loss measured.

Degradation of the copolymer is expected to occur by the hydrolysis of labile ester bonds in the polymer chains. In alkaline solutions, simvastatin is also known to hydrolyze into its active open-ring form, simvastatin α-hydroxyacid.[51] The simvastatin hydroxyacid may be included in the components resulting from breakdown, along with byproducts that may include oligosimvastatin chains, mPEG, and mPEG with minimal monomers of simvastatin attached. The hypothesized byproducts are based on the presence of ester bonds that would be present between the monomeric units and between the block components. The degradation process and products of other polyesters, such as PLGA, have been well-documented in identifying soluble oligomers that then degrade into the final products of lactic and glycolic acid in abiotic conditions.[52]

The mass spectra of the low molecular weight degradation products showed *m*/*z* values of 441 and 460, indicating the presence of simvastatin in its closed and open ring forms, respectively. The *m*/*z* values for simvastatin and simvastatin hydroxyacid have most likely been influenced by salt adducts in the analytes (*i.e.* Na^+, K^+, and H^+) because the ions are produced by cationization.[53] Salt adducts can be produced from any salts present within the sample, such as the PBS to which degradation products and simvastatin and mPEG controls were exposed before prepping the samples for MS analysis. Despite desalting the final sample solutions, a small amount of the salts remained present for detection but not nearly enough to inhibit the generation of a clear and readable spectrum. However, salt detection can still contribute to decreased ionization efficiency, which possibly influenced the increased baseline noise seen in the low molecular weight region, along with low concentration.

A parent ion value of 441 *m*/*z* is likely the result of an attachment of Na^+ (22 *m*/*z*) to the parent ion (419 *m*/*z*). A simvastatin hydroxyacid ion would gain a molar mass value of 18 due to hydrolysis, leading to an *m*/*z* value of 460, seen in the spectrum, if the salt adduct is the same as that on the parent ion with a H^+ also attached. The lower value peaks may represent a combination of fragmented ions of simvastatin,[54] the CHCA matrix (189 *m*/*z*), and salt adducts present in the sample. The same indication holds true for the peaks ranging from 490 to 693 *m*/*z* and the peak at 702 *m*/*z* in simvastatin's spectrum, along with the incorporation of ion clusters produced from the matrix[55] (*i.e.*, molecule (M): 2 M + Na^+ and 2 M + H^+ at 401 and 379 *m*/*z*, respectively) and the parent ion. The peaks of 920 and 1062 may indicate dimer ions of simvastatin along with the other combinations previously mentioned.

The pattern of peaks seen in the mPEG mass spectrum represents the repeating $–CH_2CH_2O–$ unit of the polymer. The

rightward shift in peak distribution seen in the high molecular weight degradation products indicates simvastatin monomers remaining attached to the mPEG block. Salt adducts and the presence of complex ions can lead to less defined peaks otherwise seen as a rise in the baseline under the peaks of the high molecular weight products. Thus, the mass spectral data suggests that the supernatants collected from the degrading copolymer contained a broad distribution of degradation products, including simvastatin, simvastatin hydroxyacid, dimerized simvastatin, mPEG, and mPEG with simvastatin monomers attached, some of which are possibly branched.

Despite the possibility of a branched architecture being known to accelerate degradation rates because of an increased number of end-groups present per polymer chain[56] and the large amount of water uptake of the samples within a 6 week period, limited degradation and slow simvastatin release rates were still seen within neutral and alkaline environments. This effect was attributed to the slow cleavage rate of bonded simvastatin monomers being the limiting factor and/or possible side reactions during polymerization leading to less labile bonds. Thus, investigating methods to improve the synthesis procedure to better control the ROP reaction would be beneficial in minimizing the side reaction byproducts produced in the crude copolymer.

Conclusions

A degradable poly(ethylene glycol)-*block*-poly(simvastatin) copolymer can be useful as a polymeric drug delivery system. The poly(simvastatin) block formed at and above 200 °C, showing potential for increasing the weight percentage of the prodrug in the biomaterial. ROP of simvastatin reveals a new approach for polymerizing prodrugs in the statin family and possibly in other classes of lactone-containing prodrugs that may have less steric hindrance. Less bulkiness could provide better chain propagation at more ambient reaction conditions. The minimal synthesis steps of ROP needed to polymerize prodrugs, such as simvastatin, can be desirable in scaled-up production. Although MW increased with temperature and initial degradation was observed, the rate of bond cleavage between simvastatin monomers and possible byproducts from side reactions hindered mass loss and subsequent drug release. Despite slow degradation, release of open and closed-ring simvastatin as well as simvastatin in poly(oligo)meric forms was demonstrated. By minimizing the side reactions, degradability of the mPEG-poly(simvastatin) diblock copolymer could be improved, potentially providing sufficient concentrations of simvastatin for extended treatment periods.

Acknowledgements

This research was funded in part by the NIH (AR060964-02S1, EB017902), and TAA was supported by an NSF IGERT fellowship (DGE-0653710). NMR data were obtained at the Nuclear Magnetic Resonance Facility at the University of Kentucky. Mass spectral data and help with analysis were obtained from the Mass Spectrometry Facility at the University of Kentucky.

References

1 I. Yoshito and H. Tsujh, *Macromol. Rapid Commun.*, 2000, **21**, 117–132.
2 J. C. Middleton and A. J. Tipton, *Biomaterials*, 2000, **21**, 2335–2346.
3 P. A. Gunaitllake and R. Adhikari, *Eur. Cells Mater.*, 2003, **5**, 1–16.
4 B. Dhandayuthapani, Y. Yoshida, T. Maekawa and D. S. Kumar, *Int. J. Polym. Sci.*, 2011, **2011**, 290602.
5 R. Langer, *Science*, 1990, **249**, 1527–1533.
6 N. A. Rohini, N. Agrawal, A. Joseph and A. Mukerji, *J. Antivirals Antiretrovirals*, 2013, **S15**, 7.
7 R. Duncan, *Nature*, 2006, **6**, 688–701.
8 S. S. Banerjee, N. Aher, R. Patil and J. Khandare, *J. Drug Delivery*, 2012, **2012**, 103973.
9 H. N. Joshi, *Pharm. Technol.*, 1988, **12**, 120–130.
10 R. L. Cleek, K. C. Ting, S. G. Eskin and A. G. Mikos, *J. Controlled Release*, 1997, **48**, 259–268.
11 Y. Yeo and K. Park, *Arch. Pharmacal Res.*, 2004, **27**, 1–12.
12 W. M. Saltzman and L. K. Fung, *Adv. Drug Delivery Rev.*, 1997, **26**, 209–230.
13 F. Alexis, S. S. Venkatraman, S. K. Rath and F. Boey, *J. Controlled Release*, 2004, **98**, 67–74.
14 X. Huang and C. S. Brazel, *J. Controlled Release*, 2001, **73**, 121–136.
15 A. L. Carbone and K. E. Uhrich, *Macromol. Rapid Commun.*, 2009, **30**, 1021–1026.
16 P. P. Wattamwar, Y. Mo, R. Wan, R. Palli, Q. Zhang and T. D. Dziubla, *Adv. Funct. Mater.*, 2010, **20**, 147–154.
17 R. Slivniak and A. J. Domb, *Biomacromolecules*, 2005, **6**, 1679–1688.
18 H. R. Kricheldorf, J. Kreiser-Saunders and C. Boettcher, *Polymer*, 1995, **36**, 1253–1259.
19 O. Nuyken and S. D. Pask, *Polymer*, 2013, **5**, 361–403.
20 C. P. Sparrow, C. A. Burton, M. Hernandez, S. Mundt, H. Hassing, S. Patel, R. Rosa, A. Hermanowski-Vosatka, P. Wang, D. Zhang, L. Peterson, P. A. Detmers, Y. Chao and S. D. Wright, *Arterioscler., Thromb., Vasc. Biol.*, 2001, **21**, 115–121.
21 Y. Kureishi, Z. Luo, I. Shiojima, A. Bialik, D. Fulton, D. J. Lefer, W. C. Sessa and K. Walsh, *Nat. Med.*, 2000, **6**, 1004–1010.
22 P. Y. Chen, J. S. Sun, Y. H. Tsuang, M. H. Chen, P. W. Weng and F. H. Lin, *Nutr. Res.*, 2010, **30**, 191–199.
23 E. S. Istvan and J. Deisenhofer, *Science*, 2001, **292**, 1160–1164.
24 J. R. Porter, T. T. Ruckh and K. C. Popat, *Biotechnol. Prog.*, 2009, **25**, 1539–1560.
25 R. W. Wong and A. B. Rabie, *World J. Orthod.*, 2006, **7**, 35–40.
26 J. H. Jeon, M. V. Thomas and D. A. Puleo, *Int. J. Pharm.*, 2007, **340**, 6–12.
27 T. Prueksaritanont, L. M. Gorham, B. Ma, L. Liu, X. Yu, J. J. Zhao, D. E. Slaughter, B. H. Arison and K. P. Vyas, *Drug Metab. Dispos.*, 1997, **25**, 1191–1199.

28 MRC/BHF Heart Protection Study Collaborative Group, J. Armitage, L. Bowman, R. Collins, S. Parish and J. Tobert, *BMC Clin. Pharmacol.*, 2009, **9**, 6.
29 T. D. Dziubla, A. Karim and V. R. Muzykantov, *J. Controlled Release*, 2005, **102**, 427–439.
30 J. Jing Zhang, Y. Zhao, Z. Su and G. Ma, *J. Appl. Polym. Sci.*, 2007, **105**, 3780–3786.
31 A. A. Ambike, K. R. Mahadik and A. Paradkar, *Drug Dev. Ind. Pharm.*, 2005, **31**, 895–899.
32 J. K. Tessmar and A. M. Gopferich, *Macromol. Biosci.*, 2007, **7**, 23–39.
33 K. Knop, R. Hoogenboom, D. Fischer and U. S. Schubert, *Angew. Chem., Int. Ed.*, 2010, **49**, 6288–6308.
34 M. Save, M. Schappacher and A. Soum, *Macromol. Chem. Phys.*, 2002, **203**, 889–899.
35 J. Puaux, I. Banu, I. Nagy and G. Bozga, *Macromol. Symp.*, 2007, **259**, 318–326.
36 S. Kaihara, S. Matsumura, A. G. Mikos and J. P. Fisher, *Nat. Protoc.*, 2007, **2**, 2767–2771.
37 M. Labet and W. Thielemans, *Chem. Soc. Rev.*, 2009, **38**, 3484–3504.
38 R. F. Storey, *Macromolecules*, 2002, **35**, 1504–1512.
39 G. Odian, *Principles of Polymerization*, John Wiley & Sons, Inc., Hoboken, NJ, 4th edn, 2004.
40 A. Górniak, B. Karolewicz, E. Żurawska-Płaksej and J. Pluta, *J. Therm. Anal. Calorim.*, 2013, **111**, 2125–2132.
41 C. Aleman, O. Betran, J. Casanovas, K. N. Houk and H. K. J. Hall, *J. Org. Chem.*, 2009, **74**, 6237–6244.
42 R. Ahuja, S. Kundu, A. S. Goldman, M. Brookhart, B. C. Vicente and S. L. Scott, *Chem. Commun.*, 2008, 253–255, DOI: 10.1039/b712197k.
43 J. Otera, *Chem. Rev.*, 1993, **93**, 1449–1470.
44 A. Sunder, R. Hanselmann, H. Frey and R. Mu, *Macromolecules*, 1999, **32**, 4240–4246.
45 F. Tasaka, Y. Ohya and T. Ouchi, *Macromol. Rapid Commun.*, 2001, **22**, 820–824.
46 P. J. Disjkstra, H. Du and J. Feijen, *Polym. Chem.*, 2011, **2**, 520–527.
47 V. Katiyar and H. Nanavati, *Polym. Chem.*, 2010, **1**, 1491–1500.
48 A. Duda and A. Kowalski, *Handbook of Ring-Opening Polymerization*, Wiley-VCH Verlag GmbH & Co., KGaA, Weinheim, 2009.
49 P. J. A. Veld, E. M. Velner, P. V. D. Witte, J. Hamhuis, P. J. Dijkstra and J. Feijen, *J. Polym. Sci., Part A: Polym. Chem.*, 1997, **35**, 219–225.
50 W. H. Xie, W. P. Zhu and Z. Q. Shen, *Polymer*, 2007, **48**, 6791–6798.
51 W. H. Kaesemeyer, R. B. Caldwell, J. Huang and R. W. Caldwell, *J. Am. Coll. Cardiol.*, 1999, **33**, 234–241.
52 M. Hakkarainen and A.-C. Albertsson, in *Chromatography for Sustainable Polymeric Materials*, ed. M. Hakkarainen, L. Burman, A.-C. Albertsson, M. Gröning and C. Strandberg, Springer, Verlag Berlin Heidelberg, 2008, vol. 211, pp. 85–116.
53 J. K. Lewis, J. Wei and G. Siuzdak, in *Encyclopedia of Analytical Chemistry*, ed. R. A. Meyers, John Wiley & Sons Ltd, Chichester, 2000, pp. 5880–5894.
54 H. Wang, Y. Wu and Z. Zhao, *J. Mass Spectrom.*, 2001, **36**, 58–70.
55 B. O. Keller and L. Li, *J. Am. Soc. Mass Spectrom.*, 2000, **11**, 88–93.
56 M. G. McKee, S. Unal, G. L. Wilkes and T. E. Long, *Prog. Polym. Sci.*, 2005, **30**, 507–539.

